arXiv:1405.6056v1 [hep-ph] 23 May 2014

TIFR-TH/14-15

Anomalous Triple Gauge Vertices at the Large Hadron-Electron Collider

Sudhansu S. Biswal[a,1], *Monalisa Patra*[b,2] and *Sreerup Raychaudhuri*[b,3]

[a] College of Basic Sciences, Orissa University of Agriculture and Technology, Bhubaneshwar 751 003, India.

[b] Department of Theoretical Physics, Tata Institute of Fundamental Research, 1 Homi Bhabha Road, Mumbai 400005, India.

Abstract

At a high energy *ep* collider, such as the Large Hadron-Electron Collider (LHeC) which is being planned at CERN, one can access the $WW\gamma$ vertex exclusively in charged current events with a radiated photon, with no interference from the WWZ vertex. We find that the azimuthal angle between the jet and the missing momentum in each charged current event is a sensitive probe of anomalous $WW\gamma$ couplings, and show that for quite reasonable values of integrated luminosity, the LHeC can extend the discovery reach for these couplings beyond all present experimental bounds.

Pacs Nos: 14.70.Fm, 12.60.-i, 12.15.-y, 12.20.Fv

May 26, 2014

[1] sudhansu.biswal@gmail.com [2] monalisa@theory.tifr.res.in [3] sreerup@theory.tifr.res.in

The Standard Model (SM) of elementary particle physics, originally proposed [1] in the 1960's, has achieved completion with the near-certain discovery in 2012 [2] of the long-predicted Higgs boson [3]. This became possible only because of the commissioning of the Large Hadron Collider (LHC) at CERN, Geneva, a high energy machine which runs with a greater collision energy than any of its predecessors could achieve. The LHC is currently shut down for significant upgrades in energy and luminosity intended for its next run in 2015. In the community of high energy physicists there are high expectations that in that run, or in following years, the LHC might conclusively find some signals that the Standard Model of particle physics is not the final theory, but simply an effective theory which has worked efficiently to explain the experimental results collected till date, but which will prove inadequate when we go to higher energies. In this article, we do not plan to go into the multiple reasons for such an expectation, which are well-discussed in the literature [4], but instead focus on one of the possible ways in which such signals for new physics beyond the SM could be found.

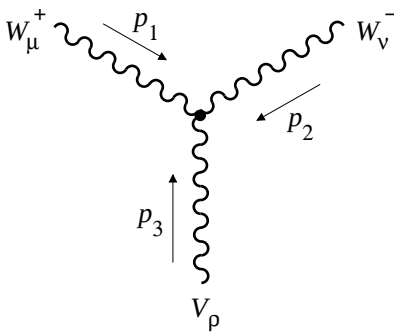

Figure 1: Illustrating momentum assignments for the generic WWV vertex.

The specific part of the SM on which we focus is one of the *triple gauge boson vertices* (TGV's) in the Standard Model — more specifically, the W^+W^-V vertex. Here V can denote any one of the neutral vector bosons γ or Z, but in this work, we focus on the specific case $V = \gamma$. In the Standard Model, of course, this vertex is precisely defined [5]. However, it is also possible to parametrise possible new physics contributions to this vertex [6] in the form of a pair of undetermined parameters $(\Delta\kappa_\gamma, \lambda_\gamma)$.

If we denote the $W^+_\mu(p_1)W^-_\nu(p_2)A_\rho(p_3)$ vertex by $i\Gamma^{(WW\gamma)}_{\mu\nu\rho}(p_1,p_2,p_3)$, then it can be neatly parametrised in the form of three separate terms, viz.

$$i\Gamma^{(WW\gamma)}_{\mu\nu\rho}(p_1,p_2,p_3) = ie\left[\Theta^{(\mathrm{SM})}_{\mu\nu\rho}(p_1,p_2,p_3) + \Delta\kappa_\gamma\Theta^{(\Delta\kappa)}_{\mu\nu\rho}(p_1,p_2,p_3) + \frac{\lambda_\gamma}{M_W^2}\Theta^{(\lambda)}_{\mu\nu\rho}(p_1,p_2,p_3)\right] \qquad (1)$$

where the Θ tensors are, respectively,

$$\begin{aligned}
\Theta^{(\mathrm{SM})}_{\mu\nu\rho}(p_1,p_2,p_3) &= g_{\mu\nu}\left(p_1-p_2\right)_\rho + g_{\nu\rho}\left(p_2-p_3\right)_\mu + g_{\rho\mu}\left(p_3-p_1\right)_\nu \qquad (2)\\
\Theta^{(\Delta\kappa)}_{\mu\nu\rho}(p_1,p_2,p_3) &= g_{\mu\rho}p_{3\nu} - g_{\nu\rho}p_{3\mu}\\
\Theta^{(\lambda)}_{\mu\nu\rho}\ (p_1,p_2,p_3) &= p_{1\rho}p_{2\mu}p_{3\nu} - p_{1\nu}p_{2\rho}p_{3\mu} - g_{\mu\nu}\left(p_{1\rho}p_2\cdot p_3 - p_{2\rho}p_3\cdot p_1\right)\\
&- g_{\nu\rho}\left(p_{2\mu}p_3\cdot p_1 - p_{3\mu}p_1\cdot p_2\right) - g_{\mu\rho}\left(p_{3\nu}p_1\cdot p_2 - p_{1\nu}p_2\cdot p_3\right)
\end{aligned}$$

This is the most general form consistent with the gauge and Lorentz symmetries of the SM [7]. The extra terms whose coefficients are $\Delta\kappa_\gamma$ and λ_γ respectively are known as the *anomalous* TGV's.

Noting that the terms in $\Theta^{(\Delta\kappa)}_{\mu\nu\rho}$ also appear in $\Theta^{(\mathrm{SM})}_{\mu\nu\rho}$, one can also combine the terms and use $\kappa_\gamma = 1 + \Delta\kappa_\gamma$, but in this paper we have used only $\Delta\kappa_\gamma$, which agrees with the common usage by most experimental collaborations.

These anomalous TGV's have been studied in some detail in many processes, both at low energies and at high energies [8]. No evidence for any deviation from the SM has been found till date, as a result of which, we have fairly stringent upper bounds on the anomalous couplings $\Delta\kappa_\gamma$ and λ_γ. The strongest bounds come from the study of W^+W^- production at the Large Electron Positron (LEP) collider at CERN, Geneva [9]. The early runs of the LHC have also yielded bounds published by both the ATLAS and the CMS Collaborations [10, 11], but these are not, as yet, competitive with the LEP bounds. A summary of the best available constraints on $\Delta\kappa_\gamma$ and λ_γ is given in Table 1.

	LEP [9]	CDF [12]	D0 [13]	ATLAS [10]	CMS [11]
$\Delta\kappa_\gamma$	[-0.099, 0.066]	[-0.460, 0.390]	[-0.158, 0.255]	[-0.135, 0.190]	[-0.210, 0.220]
λ_γ	[-0.059, 0.017]	[-0.180, 0.170]	[-0.036, 0.044]	[-0.065, 0.061]	[-0.048, 0.037]

Table 1: Allowed ranges, at 95% C.L., on the anomalous $WW\gamma$ couplings from the data collected at the LEP, Tevatron and LHC experiments. In each case, the most restrictive of the reported measurements is taken.

Although these constraints – especially the ones from the LEP data – are fairly stringent, they come with some caveats, viz. the fact that the processes used to put these bounds on the $WW\gamma$ anomalous TGV's are often affected by the WWZ anomalous TGV's. For example, if we consider the LEP process $e^+e^- \to W^+W^-$ through an s-channel photon exchange, there is also a similar process through an s-channel Z^0 exchange. The bounds quoted in Table 1 are sometimes obtained with the assumption that there are anomalous couplings in the $WW\gamma$ vertex alone, but not in the WWZ vertex, and sometimes by assuming both kinds of anomalous couplings exist and may or may not be equal. Moreover, since these anomalous couplings lead to unitarity violation at high energies, sometimes they are taken with arbitrary factors of the form $(1 + s/\Lambda^2)^\alpha$, where Λ is a high energy scale, and α is an adjustable exponent [12]. Not every experimental collaboration, however, uses these factors, and hence comparison of the different constraints could be deceptive. Further, there always remains a possibility that there may be anomalous couplings in both $WW\gamma$ and WWZ vertices such that these interfere destructively to produce a very small effect. In such a situation, many of the above bounds could be rendered invalid. A cleaner mode is the study of $W\gamma$ (or WZ) final states at a hadron collider, but this suffers from the problem of low cross sections and large SM backgrounds. Photoproduction of W and Z bosons have also been studied in the context of ep colliders like the DESY HERA [14] and the proposed CERN LHeC [15], but these do not probe very small values of the anomalous TGV couplings, and moreover, $\gamma^* \to WW$ production can easily get mixed with $Z^* \to WW$ processes.

In this context, we wish to point out that at an ep collider one can clearly distinguish between charged current (CC) events $e + p \to \nu_e +$ jet arising from W boson exchange, and neutral current (NC) events $e + p \to e +$ jet arising from photon or Z boson exchange, simply by triggering on the missing energy or the electron in the final state. Considering the CC events, if a photon is radiated from the exchanged W boson, we can trigger on a final state with a photon, one (or more) jets and missing energy. The crucial point to note is that if we trigger on a final state photon, there will be no interference from the WWZ vertex, anomalous or otherwise. Thus, if we trigger on a final state photon, an ep collider can provide very clean bounds on the anomalous TGV's and this is what is investigated in the present work.

The possible diagrams which give rise to the process $e + p \to \nu_e +$ jet in the framework of the SM are given in Fig. 2. The graph marked '1' has a red dot indicating the contribution of possible anomalous $WW\gamma$ coupling terms.

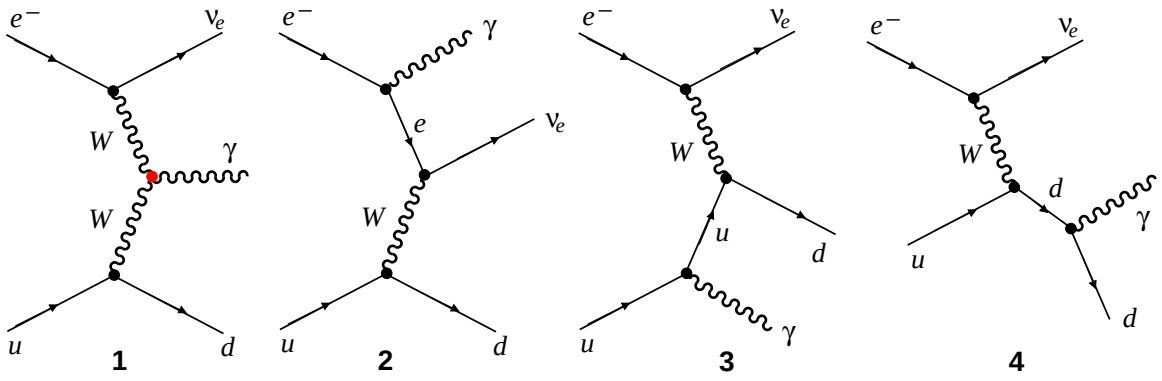

Figure 2: Feynman diagrams contributing at parton level to the process $e^- p \to \nu_e + \gamma +$ jet. The red dot in the diagram marked '1' corresponds to the anomalous TGV.

Evaluation of the diagrams in Fig. 2 leads to a matrix element of the form

$$\mathcal{M} = \mathcal{M}_0 + \Delta\kappa_\gamma \mathcal{M}_1 + \lambda_\gamma \mathcal{M}_2 \tag{3}$$

where the dominant term $\mathcal{M}_0$ is the Standard Model contribution, which arises from all four diagrams, and the trailing terms $\Delta\kappa_\gamma \mathcal{M}_1$ and $\lambda_\gamma \mathcal{M}_1$ get contributions only from the diagram marked '1'. Squaring and spin-summing/averaging this matrix element and integrating it over the accessible phase space leads, then to a parton-level cross-section of the generic form

$$\hat{\sigma} = \hat{\sigma}_{00} + \Delta\kappa_\gamma^2 \hat{\sigma}_{11} + \lambda_\gamma^2 \hat{\sigma}_{22} + \Delta\kappa_\gamma \hat{\sigma}_{01} + \lambda_\gamma \hat{\sigma}_{02} + \Delta\kappa_\gamma \lambda_\gamma \hat{\sigma}_{12} \tag{4}$$

where, in general, $\hat{\sigma}_{ij}$ arises from integration of terms of the form $\sum_s \mathcal{M}_i^\dagger \mathcal{M}_j$. Given the small values of $\Delta\kappa_\gamma$ and λ_γ allowed by the experimental data (see Table 1), it is clear that the dominant new physics contributions will come from the interference terms $\Delta\kappa_\gamma \hat{\sigma}_{01}$ and $\lambda_\gamma \hat{\sigma}_{02}$, which vary linearly with the anomalous coupling parameters $\Delta\kappa_\gamma$ and λ_γ.Thus, the main question is whether these terms can be at all significant when compared to the dominant SM term $\hat{\sigma}_{00}$.

In the most general case, the answer to the above question is clearly in the negative, since similar considerations will hold at any collider, including the CERN LEP, Fermilab Tevatron and CERN LHC, all of which have already come up with negative results for their searches (see Table 1). In fact, even if we take a differential cross-section for some kinematic variable ξ, we would still have

$$\frac{d\hat{\sigma}}{d\xi} = \left(\frac{d\hat{\sigma}}{d\xi}\right)_{00} + \Delta\kappa_\gamma^2 \left(\frac{d\hat{\sigma}}{d\xi}\right)_{11} + \lambda_\gamma^2 \left(\frac{d\hat{\sigma}}{d\xi}\right)_{22} + \Delta\kappa_\gamma \left(\frac{d\hat{\sigma}}{d\xi}\right)_{01} + \lambda_\gamma \left(\frac{d\hat{\sigma}}{d\xi}\right)_{02} + \Delta\kappa_\gamma\lambda_\gamma \left(\frac{d\hat{\sigma}}{d\xi}\right)_{12} \quad (5)$$

and any deviation of the observed deviation from the SM term (marked 00) would have been detected in the previous runs of these machines. The question is, therefore, if, in the context of the LHeC, we can (a) find some suitable variable ξ which will show appreciable deviation between the left side of Eqn. 5 and the SM term on the right, and (b) if we can devise a suitable set of kinematic cuts which will reduce the SM contribution as much as possible without affecting the $\Delta\kappa$ and λ terms too much. In pursuit of the first goal, we require to go beyond the usual transverse momentum and pseudorapidity variables and use, instead, an azimuthal angle variable, which has been used quite successfully in the literature to predict detection techniques for anomalous HWW couplings [17].

We have, of course, studied a fairly comprehensive set of the different possible kinematic variables that can be constructed using the final state particles. The one which we find most sensitive to the anomalous TGV's, especially the $\Delta\kappa_\gamma$ variable, is constructed as follows. The final state consists of an isolated hard photon and a single jet, with a substantial amount of missing transverse momentum. We now consider the transverse momenta of the jet ($\vec{p}_T^{\,\rm J}$) and the missing transverse momentum ($\not{\vec{p}}_T$) as two-dimensional vectors in the plane perpendicular to the beam axis. The angle between these vectors will be denoted by $\Delta\phi(J\not{p}_T)$ and can be constructed from

$$\cos\Delta\phi(J\not{p}_T) = \frac{\vec{p}_T^{\,\rm J}\cdot\ \not{\vec{p}}_T}{|\ \vec{p}_T^{\,\rm J}\ |\,|\not{\vec{p}}_T\ |} \quad (6)$$

We then set the variable $\xi = \Delta\phi(J\not{p}_T)$ in Eqn. 5 for the rest of our analysis. The other kinematic variables where there are differences in contribution between the SM and other terms play their part in the following kinematic cuts.

1. The emitted photon should have $p_T^\gamma \geq 50$ GeV.
2. At least one final state jet should have $p_T^{\rm J} \geq 20$ GeV.
3. The missing transverse momentum must satisfy $\not{\vec{p}}_T \geq 20$ GeV.
4. The pseudorapidities of the photon and the jet must satisfy $\eta_\gamma, \eta_{\rm J} \leq 3.5$.
5. The photon must be isolated from the jet by the criterion $\Delta R_{\gamma{\rm J}} \geq 1.5$.

Of these cuts, only the first and the last ones really function as selection cuts, since the others are practically forced upon us by the acceptance criteria of any standard detector which may be used at the LHeC [18]. However, these two cuts, which together enforce the requirement of a hard,

isolated photon, are most crucial in suppressing the SM background, the bulk of which obviously comes from bremsstrahlung processes, with their usual soft and collinear dominance.

It may be noted, at this stage, that these kinematic cuts have been specifically chosen to favour the $\Delta\kappa_\gamma$ terms in the cross-section. This is because the bounds on the λ_γ coupling are already pretty strong, whereas the bounds on $\Delta\kappa_\gamma$ are much weaker. We, therefore, seek to maximise sensitivity to the $\Delta\kappa_\gamma$ variable. It may be pointed out, that as far as kinematic cuts go, the present ones are rather moderate. Far more stringent cuts are commonly used in LHC studies — for example, in searches for supersymmetry signals one often encounters a demand that $\not{p}_T \geq 300$ GeV [19]. However, we have kept the cuts very conservative in this analysis, for two reasons. In the first place, more stringent cuts may end up by removing the entire signal, given that the LHeC integrated luminosity may not be all that high. Moreover, we find that stronger cuts on the other variables tend, in general, to reduce the difference between the SM and the anomalous TGV terms in the $\Delta\phi(J\,\not{p}_T)$ distribution. Thus, the above cuts are essentially chosen to maximise this difference, insofar as a rounding-off to standard values allows.

Some of our results are plotted in Fig. 3 for the case of a 140 GeV electron beam colliding with the 7 TeV protons from the LHC. On both the left and right panels, we have plotted the variable $\Delta\phi(J\,\not{p}_T)$ (in degrees) on the abscissa, while the ordinate represents the difference in number of events between the signal and the background. These numbers are obtained from the differential cross-section multiplied by an integrated luminosity estimated at 10^3 fb^{-1}.

In both panels of Fig. 3, the region shaded grey indicates the 95% C.L. fluctuation δN in the SM background. This is essentially flat, apart from a minor increase on the right side of the plot. The left panel, marked (a), shows the distribution when one of the couplings $\Delta\kappa_\gamma$ or λ_γ is at its maximum magnitude as permitted by the LEP constraints at 95% C.L. Thus, the solid (dashed) blue lines indicate the cases when $\lambda_\gamma = 0$ and $\Delta\kappa_\gamma = 0.066\,(-0.099)$. Similarly the solid (dashed) red lines indicate the cases when $\Delta\kappa_\gamma = 0$ and $\lambda_\gamma = 0.017\,(-0.059)$. It is clear that at 95% C.L. it will be possible to distinguish the anomalous TGV effects from the SM background for both extreme values of $\Delta\kappa_\gamma$, as well as some intermediate values which are not too small in magnitude. On the other hand, the deviation from the SM is too small for positive values of λ_γ, though when λ_γ goes negative, some deviation would be observed in the backward direction. In general, of course, both $\Delta\kappa_\gamma$ and λ_γ could have nonzero values, and the corresponding effects are illustrated in the right panel of Fig. 3, marked (b). Here the solid red (blue) lines indicate the cases when both $\Delta\kappa_\gamma$ and λ_γ have their maximum allowed negative (positive) values, as given above. In both cases there are deviations in the first quadrant, with the negative values leading to somewhat greater deviations than the positive ones.

At this point it is necessary to remember that the curves in panel (b) are not just the superposition

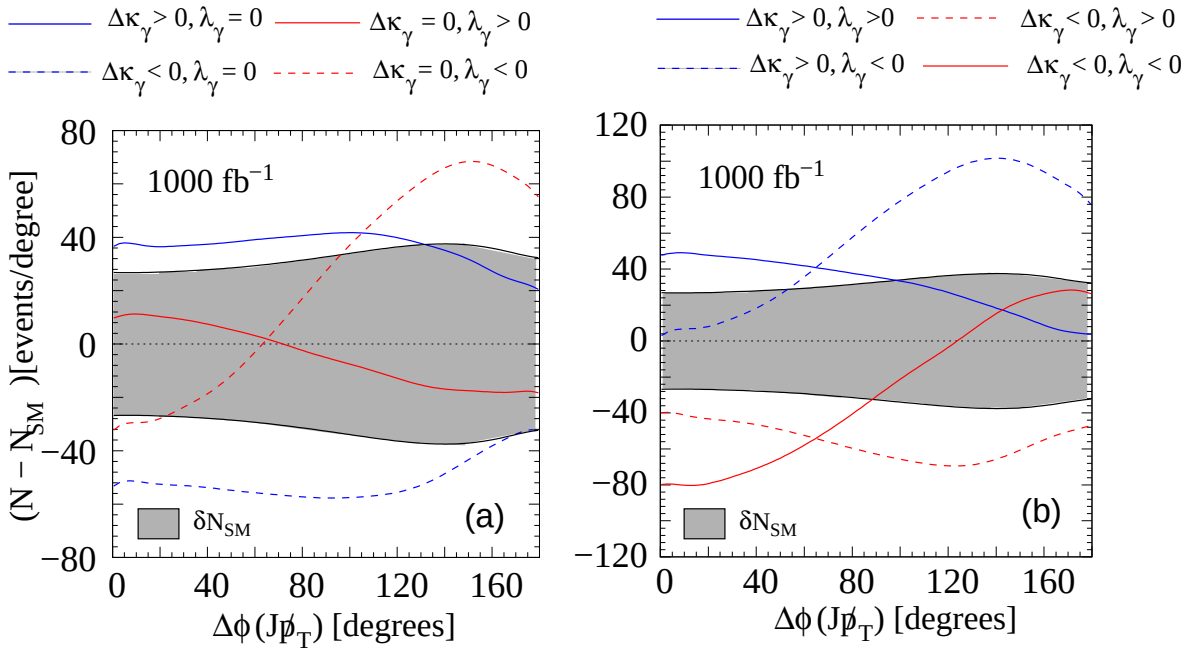

Figure 3: Distribution of the final events in the azimuthal angle difference variable $\Delta\phi(J\not{p}_T)$. In each graph on the panel on the left, marked (a), one of the parameters $\Delta\kappa_\gamma$ or λ_γ is set to zero, while the other is set to the maximum or the minimum value allowed by LEP data at the 95% C.L. level. The panel on the right, marked (b) shows similar distributions, but for the cases when both the variables have non-zero values corresponding to the maximum or minimum value allowed by LEP data at the 95% C.L. level. In both panels, the shaded region shows the 95% C.L. fluctuation in the SM background. To generate this figure, we have assumed an integrated luminosity of 10^3 fb^{-1} and an electron beam energy of 140 GeV.

of the relevant curves in panel (a) because of the interference term proportional to $\hat{\sigma}_{12}$ in Eqn. 5. When $\Delta\kappa_\gamma$ and λ_γ have opposing signs, we get greater deviations from the background, with the case $\Delta\kappa_\gamma < 0$ yielding deviations in the first quadrant, and the case $\Delta\kappa_\gamma > 0$ yielding deviations in the second quadrant. Of course, the curves shown in Fig. 3 represent only the extreme values of the anomalous couplings, as well as a highly optimistic estimate of the integrated luminosity. We thus need to set up a more sensitive criterion for distinguishability than mere inspection of a graph like Fig. 3. In order to do this, we divide the range of $\Delta\phi(J\not{p}_T)$ into 36 bins, i.e. of 5^0 each, and then calculate a $\chi^2(\Delta\kappa_\gamma, \lambda_\gamma)$ as follows

$$\chi^2(\Delta\kappa_\gamma, \lambda_\gamma) = \sum_{i=1}^{36} \frac{\left[N_i^{\rm tot}(\Delta\kappa_\gamma, \lambda_\gamma) - N_i^{\rm SM}\right]^2}{\left[\delta N_i^{\rm SM}\right]^2} \tag{7}$$

where $N_i^{\rm SM} = N_i^{\rm tot}(\Delta\kappa_\gamma = 0, \lambda_\gamma = 0)$ and, if the numbers are large enough, $\delta N_i^{\rm SM} = \sqrt{N_i^{\rm SM}}$. Since $N_i^{\rm tot}(\Delta\kappa_\gamma, \lambda_\gamma) = \mathcal{L}\sigma_i^{\rm tot}(\Delta\kappa_\gamma, \lambda_\gamma)$, where $\mathcal{L}$ is the integrated luminosity and $\sigma_i^{\rm tot}(\Delta\kappa_\gamma, \lambda_\gamma)$ is the cross-section in that bin, it follows that $\chi^2(\Delta\kappa_\gamma, \lambda_\gamma)$ varies linearly with $\mathcal{L}$. If the difference between the observed difference and the SM prediction arises from random fluctuations, we should

obtain a value of $\chi^2 \simeq 23.268$ at 95% C.L.. The criterion for a 95% C.L. discovery, then, is simply

$$\chi^2(\Delta\kappa_\gamma, \lambda_\gamma) > 23.268 \ . \tag{8}$$

The usefulness of this criterion is illustrated below, in Fig. 4. Here we have set $\lambda_\gamma = 0$ and plotted, as a function of the integrated luminosity $\mathcal{L}$, the minimum value of $\Delta\kappa_\gamma$ for which the criterion in Eqn. 8 is satisfied, i.e. the anomalous coupling $\Delta\kappa_\gamma$ is discoverable at the LHeC.

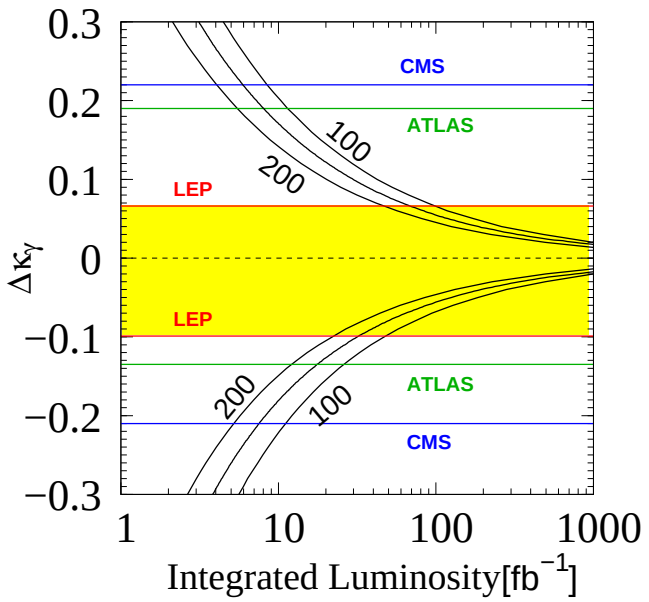

Figure 4: The 95% C.L. discovery reach of the LHeC in $\Delta\kappa_\gamma$ (assuming $\lambda_\gamma = 0$) as a function of the integrated luminosity. The best experimental bounds at 95% C.L. are as indicated on the graph. The three solid lines correspond respectively to electron beam energies of 100 GeV (marked), 140 GeV and 200 GeV (marked).

In Fig. 4, the three solid curves represent three possible energies, viz. 100 GeV, 140 GeV and 200 GeV of the electrons colliding with 7 TeV protons. As may be expected from the high momentum dependence of the anomalous couplings, we get somewhat better results with higher energy electrons than with lower energy electrons, though the difference is not all that important. On the other hand, increase of luminosity allows us to probe smaller and smaller values of $|\Delta\kappa_\gamma|$, as is apparent from the the converging lines in the figure. For comparison, we have also plotted the constraints on $\Delta\kappa_\gamma$ from the ATLAS and CMS experiments, as well as the combined LEP collaborations. The LEP bounds, which are the most restrictive, are highlighted in yellow to make the comparison easy.

It may be immediately noted that, as of now, only the LEP bounds will be comparable with the LHeC results, using the azimuthal angle variable, as soon as the integrated luminosity crosses a few tens of fb^{-1}. However, in order to better the LEP results, we will require an integrated luminosity of about 50, 70 or 100 fb^{-1} for $\Delta\kappa_\gamma > 0$ for an electron beam energy of 200, 140 or 100 GeV respectively. For $\Delta\kappa_\gamma < 0$, the corresponding values are about 25, 30 and 50 GeV respectively. Thus, we may conclude that an integrated luminosity of 100 fb^{-1}, or more, will enable the LHeC to become the most powerful probe of the anomalous TGV $\Delta\kappa_\gamma$ till now.

The graphs in Fig. 4 do not tell the whole story, however, for they represent the specific case when $\lambda_\gamma = 0$. In general, as we have seen in Fig. 3, the results will be different when both types of anomalous couplings assume non-zero values. We have, therefore, made a study of the joint variation of the χ^2 variable in Eqn. 7 with both $\Delta\kappa_\gamma$ and λ_γ varying over their allowed ranges.

Our results are illustrated in Fig. 5, where we have plotted discovery limits as contours in the plane of $\Delta\kappa_\gamma$ and λ_γ. Obviously, the black dot in the centre of the graph, which corresponds to $\Delta\kappa_\gamma = \lambda_\gamma = 0$, is the SM prediction. i.e. no anomalous TGV's.

The solid (black) contours in Fig. 5 represent the discovery reach of the LHeC, using the azimuthal angle difference variable $\Delta\phi(\mathrm{J}\,\not{p}_T)$ and the χ^2 technique of Eqns. 7 and 8. In each case the integrated luminosity, in fb^{-1}, is marked alongside the relevent contour.Regions lying between the central point $\Delta\kappa_\gamma = \lambda_\gamma = 0$ and each contour are *inaccessible* for that value of integrated luminosity. For this graph, we have assumed an electron beam energy of 140 GeV. Obviously the contours will shrink marginally if the electron energy is increased and vice versa. For comparison, we have also superposed on these contour plots the correlated 95% C.L. constraints from (*a*) the CDF and D0 Collaborations (dashes, green) at the Fermilab Tevatron, (*b*) the ATLAS and CMS constraints (dashes, blue) from the LHC, and (*c*) the LEP constraints (solid, red and shaded yellow).

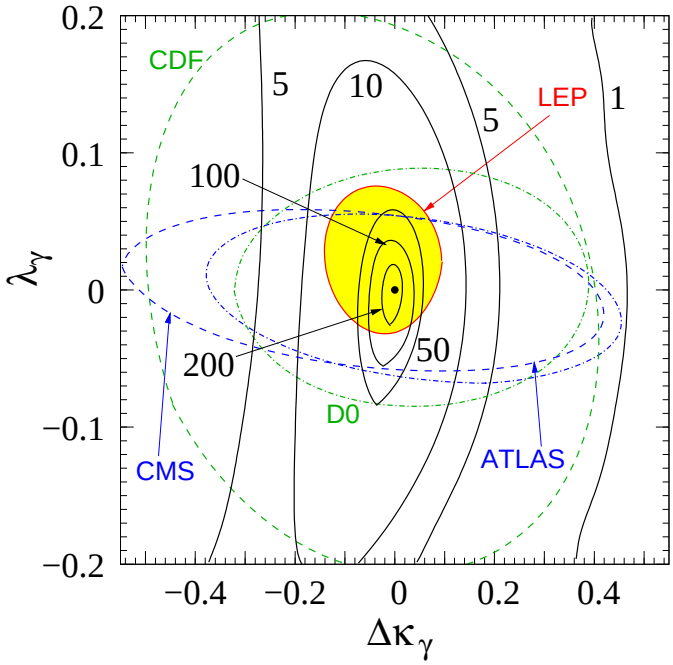

Figure 5: 95% C.L. discovery contours in the $\Delta\kappa_\gamma$–λ_γ plane corresponding to an electron beam energy of 140 GeV. The dot in the centre represents the Standard Model value. The region between this dot and each contour is *not* discoverable for the luminosity (in fb^{-1}) marked alongside the contour. The different experimental bounds at 95% C.L. are also exhibited.

It is immediately obvious from Fig. 5 that even with $\mathcal{L} = 100$ fb^{-1}, the LHeC can already access part of the parameter space which was inaccessible to the LEP and has been hitherto inaccessible at hadron colliders as well. With $\mathcal{L} = 200$ fb^{-1} it is apparent that the LHeC results will surpass all existing bounds, and it is easy to guess that the inaccessible region shrinks to really small values if the luminosity can be taken as high as $\mathcal{L} = 1000$ fb^{-1}.

In this work, therefore, we have shown that the LHeC can provide a very powerful probe of the anomalous TGV's, if we use the azimuthal angle difference variable hitherto mainly proposed to study Higgs boson physics. It is still unknown how well these discovery limits will compare with the results of the LHC, when we consider its run at 13-14 TeV and an integrated luminosity of a thousand fb^{-1} or more, for the same variable can be used to complement and enhance other studies proposed using the transverse momentum and other, more conventional distributions. Irrespective

of that, however, the LHeC has the nice feature that one can pin down the $WW\gamma$ vertex separately, and hence, this result will have no contamination from possible anomalous effects in the WWZ vertex. This, in itself, is a strong motivation to build and run the LHeC.

Acknowledgements: Some of this work was done during the 13th Workshop on High Energy Physics Phenomenology (WHEPP-13) at Puri, India, during December 2013. The work of SR is partly funded by the Board of Research in Nuclear Studies, Government of India, under project no. 2013/37C/37/BRNS.

References

[1] S.L. Glashow, Nucl. Phys. **22**, 579 (1961); S. Weinberg, Phys. Rev. Lett. **19**, 1264 (1967); A. Salam (1968) in N. Svartholm. ed. *Eighth Nobel Symposium: Stockholm* [Almquvist and Wiksell, pp. 367].

[2] G. Aad *et al.* [ATLAS Collaboration], Phys. Lett. B **716**, 1 (2012)]; S. Chatrchyan *et al.* [CMS Collaboration], Phys. Lett. B **716**, 30 (2012)]; TEVNPH Working Group (for the CDF, D0 Collaborations), Fermilab preprint FERMILAB-CONF-12-318-E, arXiv:1207.0449 [hep-ex] (2012).

[3] F. Englert and R. Brout, Phys. Rev. Lett. **13**, 321 (1964); P.W. Higgs, Phys. Rev. Lett. **13**, 508 (1964); G.S. Guralnik, C.R. Hagen, and T.W.B. Kibble, Phys. Rev. Lett. **13**, 585 (1964).

[4] For excellent reviews, see, for example, C. Quigg, Ann. Rev. Nucl. Part. Sci. **59**, 505 (2009); N. Arkani-Hamed, Phys. Scripta T **158**, 014023 (2013) ; G. Altarelli, EPJ Web Conf. **71**, 00005 (2014).

[5] See, for example, D. Bailin and A. Love, *Introduction To Gauge Field Theory*, (Taylor & Francis, UK, 1993).

[6] K. Hagiwara, R. D. Peccei, D. Zeppenfeld and K. Hikasa, Nucl. Phys. B **282**, 253 (1987).

[7] K. Hagiwara, S. Ishihara, R. Szalapski and D. Zeppenfeld, Phys. Lett. B **283**, 353 (1992) and Phys. Rev. D **48**, 2182 (1993); M. N. Dubinin and H. S. Song, Phys. Rev. D **57**, 2927 (1998).

[8] H. Aihara et al., *Electroweak symmetry breaking and new physics at the TeV scale* (Ed. T. L. Barklow et al) pp. 488-546 (1995), [arXiv:hep-ph/9503425], and references therein; J. Ellison and J. Wudka, Ann. Rev. Nucl. Part. Sci. **48**, 33 (1998).

[9] S. Schael *et al.* [ALEPH, DELPHI, L3, OPAL and LEP Electroweak Collaborations], Phys. Rept. **532**, 119 (2013).

[10] G. Aad *et al.* [ATLAS Collaboration], Phys. Rev. D **87**, 112001 (2013) and Phys. Rev. D **87**, 112003 (2013).

[11] S. Chatrchyan *et al.* [CMS Collaboration], Eur. Phys. J. C **73**, 2610 (2013) and arXiv:1308.6832 [hep-ex].

[12] T. Aaltonen *et al.* [CDF Collaboration], Phys. Rev. D **76**, 111103 (2007).

[13] V. M. Abazov *et al.* [D0 Collaboration], Phys. Lett. B **718**, 451 (2012).

[14] G. Couture, S. Godfrey and P. Kalyniak, Phys. Rev. D **39**, 3239 (1989); U. Baur and D. Zeppenfeld, Nucl. Phys. B **325**, 253 (1989); C. S. Kim and W. J. Stirling, Z. Phys. C **53**, 601 (1992); T. Helbig and H. Spiesberger, Nucl. Phys. B **373**, 73 (1992); C. S. Kim, J. Lee and H. S. Song, Z. Phys. C **63**, 673 (1994); S. Atag and I. T. Cakir, Phys. Rev. D **63**, 033004 (2001).

[15] C. Brenner Mariotto and M. V. T. Machado, Phys. Rev. D **86**, 033009 (2012).

[16] U. Baur and M. A. Doncheski, Phys. Rev. D **46**, 1959 (1992); S. Godfrey, Z. Phys. C **55**, 619 (1992).

[17] T. Plehn, D. L. Rainwater and D. Zeppenfeld, Phys. Rev. Lett. **88**, 051801 (2002); S. S. Biswal, R. M. Godbole, B. Mellado and S. Raychaudhuri, Phys. Rev. Lett. **109**, 261801 (2012).

[18] J. L. Abelleira Fernandez *et al.* [LHeC Study Group Collaboration], J. Phys. G **39**, 075001 (2012)

[19] See, for example, S. Chatrchyan *et al.* [CMS Collaboration], Eur. Phys. J. C **73**, 2568 (2013).